

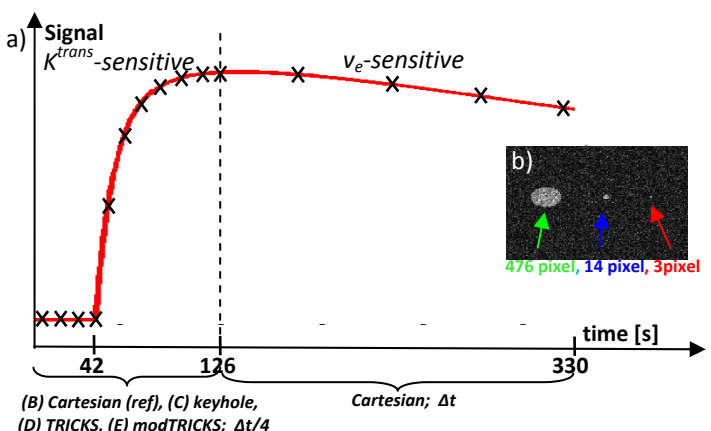
Analysis of signal-adaptive k-space acquisition schemes in quantitative dynamic contrast-enhanced MRI

I. N. Kompan^{1,2}, C. Prieto³, B. R. Knowles⁴, H. Laue¹, G. Charles-Edwards³, M. Guenther^{1,2}, and T. Schaeffter³

¹Fraunhofer MEVIS-Institute for Medical Image Computing, Bremen, Germany, ²Faculty of Physics and Electronics, University of Bremen, Bremen, Germany, ³Division of Imaging Sciences, King's College London, St. Thomas' Hospital, London, United Kingdom, ⁴Cardiovascular Division, Beth Israel Deaconess Medical Center, Harvard School of Medicine, Boston, MA, United States

INTRODUCTION: Dynamic contrast-enhanced (DCE) MRI is widely used in oncology for diagnosis and monitoring of response to treatment, particularly for novel anti-angiogenic based therapies [1]. Pharmacokinetic (PK) modelling can be applied to these data to produce quantitative parameters that reflect the underlying vasculature, as the interstitial space and the vascular permeability K^{trans} , which has been highlighted as being particularly important [2]. For an accurate fit of the PK model, high temporal resolution is required [3]. However, high spatial resolution is desirable to depict PK variations within a heterogeneous lesion. Using simulated phantom data, this work investigates the accuracy of K^{trans} fitting to signal-adaptive acquisition schemes that employ higher temporal/lower spatial resolution during the K^{trans} -sensitive initial uptake of contrast agent and lower temporal/higher spatial resolution during wash-out to maintain good visualisation of the lesion. To increase temporal resolution during the upslope phase, different k-space sampling strategies were employed and their influence on K^{trans} was studied.

METHODS: Using a numerical phantom containing 3 ROIs of different sizes (fig. 1.b), a series of proton density (PD) weighted and T_1 -weighted gradient echo DCE-MR images (TR=3.4 ms and flip angles of $\theta_{pdw} = 12^\circ$, $\theta_{tw} = 2^\circ$, respectively) were generated using the Tofts model [4] with $K^{trans} = 0.36 \text{ min}^{-1}$ and $v_e = 0.34$. For all $T_{1,0} = 900$ ms and a population-averaged arterial input function [5] was assumed. Noise was added to give SNRs of 10 and 20. The conversion from signal intensity to concentration was achieved via T_1 acquisition schemes were simulated (Fig 1.a). For all schemes, a fully sampled Cartesian acquisition with high spatial resolution was used after reaching the peak of the Signal Time Curve (STC). Before the peak, the following schemes were tested: (A) fully sampled Cartesian leading to equidistant sampling during the whole STC (for comparison with the accelerated schemes), (B) currently physically not possible reference case of fully sampled Cartesian with increased temporal resolution by a factor of 4 in comparison to the v_e -sensitive part after the peak. Before the peak different schemes, keyhole, TRICKS, modTRICKS and Cartesian (reference) are employed to accelerate imaging, after the peak fully sampled Cartesian acquisition is used.



(B) Cartesian (ref), (C) keyhole,

Cartesian; Δt

(D) TRICKS, (E) modTRICKS; $\Delta t/4$

Fig. 1.a) Signal time curve based on the Tofts model. During the K^{trans} -sensitive part of the curve, temporal resolution is increased by a factor of 4 in comparison to the v_e -sensitive part after the peak. Before the peak different schemes, keyhole, TRICKS, modTRICKS and Cartesian (reference) are employed to accelerate imaging, after the peak fully sampled Cartesian acquisition is used.

b) Resolution phantom with 3 ROIs of sizes 476, 14 and 3 pixels.

calculation using PD- and T_1 -weighted images. Five different temporal k-space acquisition schemes were simulated (Fig 1.a). For all schemes, a fully sampled Cartesian acquisition with high spatial resolution was used after reaching the peak of the Signal Time Curve (STC). Before the peak, the following schemes were tested: (A) fully sampled Cartesian leading to equidistant sampling during the whole STC (for comparison with the accelerated schemes), (B) currently physically not possible reference case of fully sampled Cartesian with increased temporal resolution by a factor of 4 in comparison to the v_e -sensitive part after the peak. Before the peak different schemes, keyhole, TRICKS, modTRICKS and Cartesian (reference) are employed to accelerate imaging, after the peak fully sampled Cartesian acquisition is used. The Tofts model was fitted to the mean concentration time curves within the ROIs. The resulting PK parameters were compared to the input values and their ratios K^{trans}_{rel} and v_e_{rel} were calculated. For each Δt this procedure was repeated 30 times and the mean of the resulting K^{trans}_{rel} was plotted against temporal resolution with error bars showing the standard deviation.

RESULTS:

SNR20 Equisistant Cartesian (A)

Cartesian (Reference) (B)

Keyhole-Cartesian (C)

TRICKS-Cartesian (D)

modTRICKS-Cartesian (E)

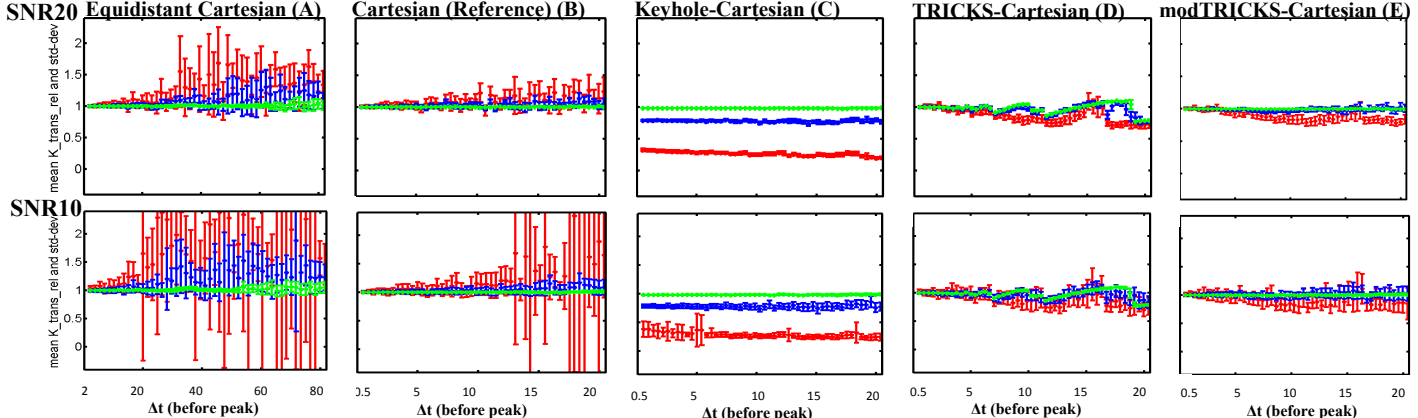


Fig. 2: Relative K^{trans} versus temporal resolution for different acquisition schemes of 3 ROIs for SNR 10 and 20. Legend: green = ROI of size 476 pixels, blue = ROI of size 14 pixels, red = ROI of size 3 pixels. Δt (before peak) describes the temporal resolution during the K^{trans} -sensitive part of the curve. The temporal resolution during the v_e -sensitive part of the curve is 4 times lower, respectively (not shown in graph). Error and standard deviation increase with decreasing ROI size for each scheme. Employing adaptive schemes reduces the standard deviation, however scheme dependent systematic errors occur. Scheme (E) displays best accuracy of relative K^{trans} values.

The results can be seen in Figure 2. In general it can be seen that with decreasing ROI size the standard deviation and systematic errors increase. The comparison of schemes (A) and (B) shows that sampling more data points during the baseline and the uptake of contrast agent scales down K^{trans} overestimation and standard deviation. The physically possible schemes (C), (D) and (E) reduced the standard deviation as well, but different systematic errors occur. Employing scheme (C) leads to increasing underestimation of K^{trans} with decreasing ROI size. For TRICKS (D) abrupt changes can be seen which arise from false onset estimation [7] and linear interpolation during the time period of the onset. ModTRICKS (E) shows the smallest systematic errors for all ROIs, however an underestimation of K^{trans} for the smallest ROI can be detected. Errors of v_e did not exceed 15%, therefore only the results of K^{trans} are displayed.

DISCUSSION: The effects of different signal adaptive k-space acquisition techniques on PK modelling were simulated. It could be shown that the acceleration of imaging during baseline and initial uptake with fully sampled image quality clearly reduces systematic errors and standard deviation. For all schemes, standard deviation and systematic errors increased with decreasing ROI size. Accelerating using keyhole shows significant systematic errors, particularly for small ROIs, due to the fact that higher k-space frequencies are not updated. For TRICKS linear interpolation of k-space-centre data leads to fit errors especially in the area of the onset, while modTRICKS partly corrects for these by updating a small section of k-space centre with every dynamic frame. In conclusion, for all investigated temporal resolutions employing scheme (E) improves the accuracy of K^{trans} most, but still leading to underestimation of K^{trans} of ~20% for small ROIs and low temporal resolutions. In the next step the tool could be applied to investigate if there are even more suitable schemes, i.e. radial or spiral imaging and select the most appropriate sequence on the scanner to apply the investigated methods *in vivo*.

REFERENCES: [1] A. Jackson, et al, Springer, 2005; [2] Leach, et al, British Journal of Cancer 2005; 92: 1599-1610; [3] Henderson, et al, MRI 1998; 16:1057-1073; [4] Tofts, et al, MRM 1991; 17: 357-367; [5] Simon Walker-Samuel, PhD Thesis, University of London, 2007; [6] F.R. Korosec, et al, MRM 1996; 36: 145-351; [7] H. Laue, et al, ISMRM 2010